

DEM accuracy evaluation in mountain area by utilizing topographic corrected products of high-resolution TerraSAR-X data

NONAKA, Takashi^{1*} ; OKAJIMA, Yuki¹ ; TSUKAHARA, Koichi¹

¹PASCO CORPORATION

The commercial high-resolution Synthetic Aperture Radar (SAR) sensors have been developed during past few years and became essential source of information in Earth Observation. The production of the maps is examined in the various fields, such as the damaged area caused by disaster, paddy field area, and forest etc. The interpretation of the objects from the images and the positional accuracy of the images are highly important for the map creation and several basic studies for such issues are also conducted by applying high-resolution SAR data.

TerraSAR-X is one of the commercial SAR satellites, and has acquired data worldwide after it was launched in June 2007. Furthermore, TanDEM-X (TerraSAR-X add-on) was launched in 2010. Both satellites are currently acquiring land surface of Earth for creating global and homogeneous Digital Elevation Model (DEM) of very high precision. TerraSAR-X has several processing level products, and the Geocoded Enhanced Ellipsoid Corrected (EEC) is amplitude data projected to the digital elevation model (DEM), which makes possible for users to integrate other optical data and GIS data. Pre-geocoded Single Look Slant Range Complex (SSC) product is complex data with two axes in the azimuth-slant range plane, and used for interferometric and polarimetric analysis.

It was reported that the geometric accuracy of SSC product was better than 1 m in several previous studies, however there are no reports stating details for the validation results of the EEC product using the actual TerraSAR-X data though it is utilized by the most of users. Therefore the authors evaluated the geometric accuracy of the EEC product by performing in-situ experiment using reflectors on the flat area, simultaneously conducted during satellite passed over. The results showed that the accuracy satisfied several meters in case of utilization of SRTM DEM. In the next stage, we developed the model showing the relationships between the geometric accuracy of range direction, DEM accuracy, incidence angle, and it was revealed that the accuracy of the model was about 1 m in the flat area.

The purpose of this study was to evaluate the accuracy of utilized DEM for the topographic correction by applying the model to TerraSAR-X data in the mountain area. The utilized TerraSAR-X data were 2 data sets of high-resolution SpotLight mode (about 2 m resolution) with the different incidence angles, and the DEMs were produced by ASTER with the mesh of 30 m and SRTM with 90 m. We also used the airborne optical data with a geometric accuracy (Digital topographic level of 2,500 scales) for a validation.

Firstly we selected 25 validation points from the intersections and curves of roads easily interpreted both from TerraSAR-X and airborne data. The average, standard deviation, and Root Mean Square Errors (RMSE) value of the difference between TerraSAR-X and reference optical data were evaluated for X-, Y-, and X-Y plane. In the next stage, we examined to apply the model to data in the mountain area. We estimated DEM's errors by assuming that the variation of the differences of the X-direction was corresponded to the errors of the topographic correction since the range direction was almost same for X direction. The results were summarized based on the evaluations of both flat and mountain areas.

Keywords: Geometric accuracy, TerraSAR-X, topographic correction, ASTER, SRTM

Pi-SAR-L2 observation of the landslide caused by Typhoon Wipha on Izu Oshima island

WATANABE, Manabu^{1*} ; DAN, Risako² ; MOTOHKA, Takeshi¹ ; OHKI, Masato¹ ; SHIMADA, Masanobu¹

¹Japan Aerospace Exploration Agency, ²RESTEC

On October 16, 2013, Typhoon Wipha struck Izu Oshima island, and a large-scale landslide was induced by the heavy rain. Six days after the disaster, Pi-SAR-L2 observation was carried out in four different observation directions (L203201?L203204). One Pi-SAR-L observation (L03801) was carried out before the disaster on August 30, 2000 in same observation direction of L203201. The observation data were used to determine which parameters and directions are preferable to detect landslide areas. Several full polarimetric parameters, including Sigma₀, polarimetric coherence, four-component parameters, and eigenvalue decomposition parameters were obtained using PolSARPro and a self-produced programs. As pointed out by Shimada et al. [1], the change of the land cover from a forest before the disaster to bare soil after the disaster was well detected by the coherence between HH and VV. In addition to this parameter, the eigenvalues and four-component decomposition parameters have the potential to detect landslide areas. The data from observations of the bottom to the top of the landslide detect the landslide well, whereas the observation of the opposite side are not as useful.

Soil from the landslide intruded into the town areas, but none of the full polarimetric parameters show any significant difference between the landslide-affected town areas and the unaffected areas.

[1] Masanobu Shimada, Manabu Watanabe, Noriyuki Kawano, Masato Ohki, Takeshi Motooka, and Yutaka Wada, Detecting Mountainous Landslides by SAR polarimetry: A Comparative Study Using Pi-SAR-L2 and X band SARs, Transactions of the Japan Society for Aeronautical and Space Sciences, Aerospace Technology Japan, 2014, 12, No.ists29, pp. Pn9-Pn15.

Keywords: Full polarimetry, SAR, disaster

Shoreline change analysis using JERS-1/SAR and ALOS/PALSAR amplitude images

ASAKA, Tomohito^{1*} ; IWASHITA, Keishi¹ ; KUDOU, Katsuteru¹ ; AOYAMA, Sadayoshi¹ ; SUGIMURA, Toshiro²

¹Nihon University, ²Remote Sensing Technology Center of Japan

Aerial photo analysis and bathymetric survey are commonly conducted to investigate the actual conditions and temporal variation in beach transformation. In recent years, satellite-based optical imagery has been more widely used to evaluate coastal erosion. However, defining shoreline edges using optical imagery is difficult because the sand under seawater near the shoreline can often be seen through clear water. On the other hand, synthetic aperture radar (SAR) imagery can be used to interpret the boundary between a sandy beach and seawater; this is possible because the incident radio waves are not transmitted through water, and SAR images can be compared to trace the shoreline. In this work, we examine the potential of shoreline change analysis by using Japanese Earth Resources Satellite 1 (JERS-1)/SAR and Advanced Land Observing Satellite/Phased Array type L-band Synthetic Aperture Radar (ALOS/PALSAR) amplitude images. We consider Kuji?kurihama beach in Chiba Prefecture as our test site; along this beach, the shoreline is almost perpendicular to the SAR antenna beam orientation for the descending orbit.

We propose a three-step automated shoreline-tracing method to assess the temporal variation of the shoreline in the study area; the HH-polarized JERS-1/SAR amplitude image captured on February 22, 1993, and the HH-polarized ALOS/PALSAR amplitude image captured on May 20, 2010 were used for this purpose. In our method, a shoreline is traced as vector data. In the first step, edge pixels in SAR images are identified by using the Laplacian of a Gaussian filter. In the second step, unwanted edge pixels are masked on the basis of a discriminant analysis in which candidate shoreline edge pixels are estimated by using statistical information within a moving window. The criteria for identifying shoreline edge pixels is decided on the basis of previously gathered data, the backscattering average, and the standard deviation, in the training area (30 by 10 pixels) encompassing the sea, shoreline, and land. In the third step, shoreline vector data are generated from continuous candidate shoreline edge pixels by an automated shoreline-tracing algorithm.

The results were verified in two ways. We first verified the location of the shoreline edge in the SAR amplitude images by overlaying multispectral images acquired on dates close to the acquisition dates of the earlier mentioned JERS-1/SAR data and ALOS/PALSAR data: the JERS-1/Optical Sensor (OPS) color composite image acquired on May 3, 1993, and the ALOS/Advanced Visible and Near Infrared Radiometer type 2 (AVNIR-2) color composite image acquired on January 8, 2011, were used for this analysis. Next, we calculated the statistical information of the backscattering data in the JERS-1/SAR and the ALOS/PALSAR amplitude images for our selected training area. It is noteworthy that the backscattering average and standard deviation in the shoreline training area is a unique than anything training area.

Our proposed method reproduces the temporal variation of the shoreline by using JERS-1/SAR and ALOS/PALSAR amplitude images. However, a part of the shoreline extracted using the JERS-1/SAR amplitude image was inaccurate. The speckle noise in the JERS-1/SAR amplitude image and the low spatial resolution of the raw data may have caused these errors. In our future work, we intend to improve the algorithm for JERS-1/SAR data and accumulate backscattering information of shoreline edge areas using SAR amplitude images.

Keywords: backscattering, beach erosion

Glacier observations by airbourne synthetic aperture radar, PiSAR2, at Tateyama, Japan

FURUYA, Masato^{1*} ; FUKUI, Kotaro² ; SUGIYAMA, Shin³ ; SAWAGAKI, Takanobu⁴

¹Hokkaido University, Graduate School of Science, ²Tateyama Caldera Sabo Museum, ³Institute of Low Temperature Science, ⁴Hokkaido University, Graduate School of Environmental Science

Fukui and Iida (2012) reported that three snowy gorges at Tateyama, Japan, were flowing at a rate of 10-30 cm/month and hence could be identified as glaciers. Fukui and Iida's observations are based on ground-based GPS observations. Because glacier flow velocity data sets are one of the fundamental physical quantities to better understand the dynamics, conventional geodetic techniques have been applied, and the measurement accuracy has significantly improved. However, due to the severe environment and logistic problems, SAR-based velocity mapping has been performed with successful results at large glaciers and ice sheets over the past decades. The velocity mapping technique is so called pixel-offset (or feature) tracking. Thus, applying the same technique to the fore-mentioned newly discovered glaciers, we should also be able to detect the spatial distribution of glacier velocities. However, the presently available satellite-based SAR data set does not have enough spatial resolutions to resolve the velocities. In this regard, the 30-cm resolution of Pi-SAR2 seems promising to perform the pixel-offset tracking. Here we report the first observation images of the Japanese glaciers acquired by Pi-SAR2, and will discuss the preliminary report of velocity mapping.

Keywords: SAR, glacier, Tateyama

Monitoring of Ice sheet marginal zone using multi-frequency SAR data

YAMANOKUCHI, Tsutomu^{1*} ; DOI, Koichiro² ; NAKAMURA, Kazuki³ ; AOKI, Shigeru⁴

¹Remote Sensing Technology Center of Japan, ²National Institute of Polar Research, ³Nihon University, ⁴Institute of Low Temperature Science, Hokkaido University

Environment of Antarctic continent and ice sheet marginal zone is quite important for understanding the mass balance of ice, formation of deep ocean water and other cryospheric phenomena. Previous study showed the usefulness of SAR data to understand what is happen on the boundary area between ice sheet and ice shelf by SAR data analysis, and achieved the mapping of ice sheet surface velocity mapping. In recent, many kinds of satellite equipped SAR sensor plan to launch and these data are available through the scientific Research Announcement (RA) or Announcement of Opportunity (AO).

Based on these facts, this study focuses on the use of multi-frequency SAR data for ice sheet marginal zone monitoring. Especially, we focus on the use of InSAR analysis for grounding line extraction, ice flow velocity mapping by offset tracking, and understanding the image feature difference through the interpretation of X-, C- and L- band SAR data. We use X-band data by TerraSAR-X, C-band data by ENVISAT and ERS-1/2, and L-band data by ALOS/PALSAR data. Then, we will try to describe the applicability and prospectives of ALOS-2 / PALSAR-2 data

TerraSAR-X data were provided by DLRs' AO project (Proposal No. HYD1808), ERS-1/2 and ENVISAT data were provided by ESA Cat-1 AO project, (project CIP.7657) and ALOS/PALSAR data were provided by Research Announcement by JAXA PI project (PI No. P1418002).

Keywords: Ice sheet, multi-frequency, SAR

Evaluation of surface roughness, magnetic permeability and dielectric permittivity using polarimetric SAR data

KOIKE, Katsuaki^{1*} ; MASUDA, Takayuki¹ ; SAEPULOH, Asep² ; URAI, Minoru³ ; OMURA, Makoto⁴ ; DOI, Koichiro⁵

¹Graduate School of Eng., Kyoto Univ., ²Bandung Institute of Technology, ³Geological Survey of Japan, AIST, ⁴Dept. Cultural Studies, Univ. Kochi, ⁵National Institute of Polar Research

Synthetic Aperture Radar (SAR) systems have great advantages of observing the Earth surface regardless of meteorological conditions and detecting crustal deformations by Interferometric processing. Another latest technique, polarimetric SAR has also been widely used through its principle that backscattering intensity differs with polarization mode. However, most applications are limited to image classification. In addition, the evaluation method for surface physical properties has not yet been investigated well. To achieve this evaluation from the viewpoints of geological identification and water-content estimation of soils, this study adopts mdPSAR (**m**agnetic permeability and **d**ielectric permittivity from **P**olarimetric **S**ynthetic **A**erture **R**adar) proposed by Saepuloh *et al.* and tries to evaluate roughness, relative magnetic permeability, and relative dielectric permittivity of the surface materials using the HH, VV, and HV mode SAR data.

As the first step of mdPSAR, the surface roughness is calculated from the backscattering coefficient data at the HV mode and an empirical equation based on an assumption of fractal property of the topography (Campbell and Shepard, 1996). Next, using the Small Perturbation Model (Fung and Chen, 2010) of backscattering coefficient and the Nelder-Mead Simplex method (a method of nonlinear optimization), the relative magnetic permeability and the relative dielectric permittivity are calculated by minimizing the difference between the model and the backscattering coefficient data at the HH and VV modes.

The areas around the Tottori sand dunes were selected as a case study of mdPSAR using two scenes of ALOS PALSAR data acquired on 25 October and 27 April 2009. As the result, the average calculation errors were small as about 1% for both the HH and VV modes and the errors were uniform in general over the scenes. The relative dielectric permittivity values of the Tottori sand dunes were evaluated as 13.4 and 10.6. These values correspond with those of wet sands. It is noted that the value is higher in the scene after raining. Higher values of relative magnetic permeability were evaluated in the sand dunes than the surroundings, which is a reasonable trend because the sands are originated from the weathering of granitic rocks containing magnetite. Consequently, the effectiveness of mdPSAR is demonstrated. However, an improvement is necessary for the surface-roughness estimation of the areas occupied by artificial structures such as buildings. This is because the HH mode intensity becomes strong in them.

Application of mdPSAR to the PARSAR data around Syowa Station, Antarctica is in progress. Its purposes are to clarify distribution of outcrops and snow ice areas, melting state of ices, and development of crevasse topography from the spatio-temporal changes of surface roughness and relative dielectric permittivity.

References

Campbell, B.A., Shepard, M.K. (1996) Lava flow surface roughness and depolarized radar scattering, *J. Geophys. Res.*, v. 101 (E8), 18941-18951.

Fung, A.K., Chen, K.S. (2010) *Microwave Scattering and Emission Models for Users*, Artech House, Norwood, MA.

Saepuloh, A., Urai, M., Koike, K., Sumantyo, J.T.S.: An advanced technique to identify surface materials on an active volcano by deriving magnetic permeability and dielectric permittivity from polarimetric SAR data, *IEEE Geosci. & Remote Sens. Lett.* (under review)

Keywords: ALOS PALSAR, polarization mode, backscattering coefficient, nonlinear optimization, Tottori sand dunes

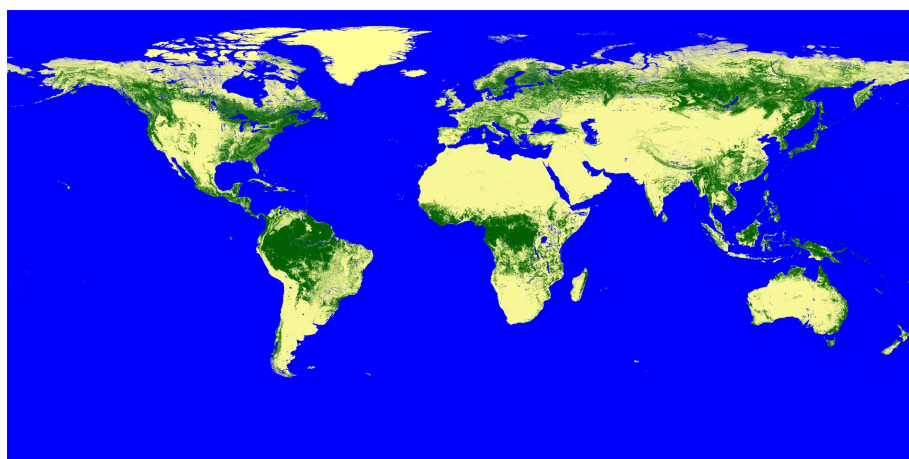
New Global Forest/Non-Forest Maps from ALOS PALSAR data (2007-2010)

SHIMADA, Masanobu^{1*} ; ITOH, Takuya² ; WATANABE, Manabu¹ ; MOTOOKA, Takeshi¹ ; RAJESH, Thapa¹

¹Japan Aerospace Exploration Agency, ²Remote Sensing Technology center of japan

Four global mosaics of Advanced Land Observing Satellite (ALOS) Phased Arrayed L-band Synthetic Aperture Radar (SAR) HH and HV polarization data were generated at 25 m spatial resolution using data acquired annually from 2007 to 2010. Variability in L-band HH and HV gamma-naught for forests was observed between regions, with this attributed to differences in forest structure and vegetation/surface moisture conditions. Region-specific backscatter thresholds were therefore applied to produce from each annual mosaic, a global map of forest and non-forest cover from which maps of forest loss and gain were mapped. Using a combination of Degree Confluence Project (DCP), Forest Resource Assessment (FRA) and Google Earth images as ground data, the overall agreement was 85 %, 91 % and 95 % respectively. Using 2007 as a baseline, decreases of 0.040 and 0.028 dB (with a 0.006 dB confidence level) were observed in the HH and HV gamma-naught respectively suggesting a decrease in forest area and increased smoothing of the global surface at the L-band radar observation. The maps provide a new global resource for documenting the changing extent of forests and contributing to ongoing monitoring through integration with historical (1992-1998) Japanese Earth Resources Satellite (JERS-1) SAR and forthcoming (from 2014) ALOS-2 PALSAR-2 data.

Keywords: SAR, forest/non-forest, SAR mosaic



Recent progress in InSAR and PolSAR signal processing

HIROSE, Akira^{1*}

¹The University of Tokyo

This invited talk reviews latest technology in synthetic aperture radar (SAR) signal processing, in particular interferometric SAR (InSAR) and polarimetric SAR (PolSAR), by focusing on the works on adaptive processing made by the author's group. This field attracts more attention because of its usability in solving serious social problems through, e.g., disaster monitoring and mitigation, water resource management, and prevention of global warming. We discuss a radar-physics-based adaptive processing framework, namely complex-valued neural networks, to increase variety of observation functions and/or improve the accuracy. We also introduce a new phase-unwrapping method to discuss its recent progress.

Keywords: synthetic aperture radar, interferometry, polarimetry, complex-valued neural network, phase unwrapping, Singularity-spreading phase unwrapping

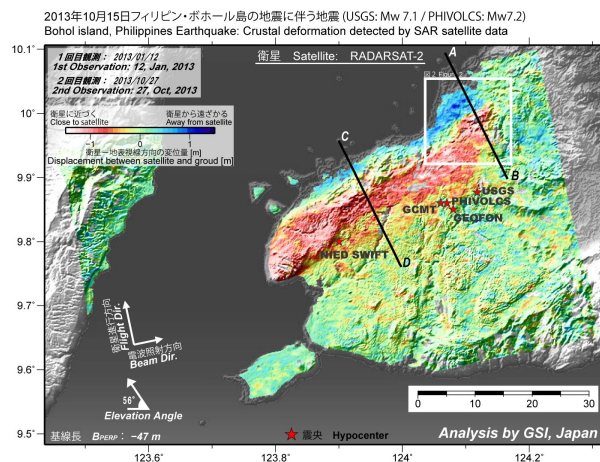
Uplift and reverse fault rupture of the 2013 Bohol earthquake (Mw 7.2), Philippines, revealed by SAR pixel offset analysis

KOBAYASHI, Tomokazu¹ ; TOBITA, Mikio^{1*}

¹GSI of Japan

Applying a pixel offset analysis using RADARSAT-2 SAR data to an inland crustal earthquake that occurred in Bohol Island, Philippines on 15 October, 2013, we succeeded in mapping a ground displacement associated with the earthquake. The most concentrated crustal deformation is located in the northwest of the island with ground displacement exceeding 1 m. The crustal deformation is zonally distributed with the length of approximately 50 km in the ENE-WSW direction. The ground in the mountainous area moves toward the satellite, while in the northern coastal zone the ground moves away from the satellite. A clear displacement discontinuity with the length of about 5 km, probably corresponding to earthquake surface faults, can be identified in the northeastern part. Our fault model that consists of two rectangular planes shows nearly pure reverse fault motions on south-southeast-dipping planes with moderate dip angles. A local rupture located in the northeast occurs at shallow depths, causing appearance of surface ruptures. Applying an additive color process using SAR amplitude images, significant changes in the backscatter intensity are detected along the coast from Maribojoc to Loon, suggesting that the seafloor uplifted and the shoreline shifted seaward resultantly. The area showing the shoreline change is in good spatial agreement with the locally-distributed large ground uplift predicted from our fault model. We can identify a good correlation between the ground upheaval produced by the reverse fault motion and the elevation in the mountainous area, consistent with the idea that the historically-repeated reverse faultings have developed the present-day topography.

Keywords: Bohol earthquake, Crustal Deformation, Pixel offset analysis, uplift, SAR, RADARSAT-2



Estimate of error in ALOS/PALSAR interferograms

HASHIMOTO, Manabu^{1*}

¹DPRI, Kyoto University

Large deformation is generated by the subduction of the Philippine Sea plate in Shikoku. GNSS observation reveals a WNW ward horizontal motion and a velocity gradient from south to north. This velocity field is suitable for the observation with SAR, which is sensible to the E-W ward displacement field. Based on these facts, we have conducted to derive average velocity in Shikoku using ALOS/PALSAR. We mainly analyzed ascending images acquired during 4 years, but anomalously large displacements (peak-to-peak displacement ~ 50 cm) were often observed possibly due to ionospheric disturbances. We discarded interferograms with such disturbances with visual inspection, and stacked rest of them. However we found E-W velocity gradient in Shikoku that is inconsistent with GNSS observations, when stacked interferograms are superposed from 4 paths. Furthermore, discontinuities between paths are evident in the Chugoku district. Therefore we made error estimate in order to clarify its magnitude and spatial distribution, comparing line-of-sight displacements derived from InSAR and GNSS.

The procedure is as follows:

(1) Calculate displacements of GNSS stations between the acquisitions of master and slave images for a specific pair from the F3 solution of GEONET and convert them to LOS displacements.

(2) Extract LOS displacements at GNSS sites from the interferogram.

(3) Take differences of LOS displacements between interferogram and GNSS.

(4) Examine dependence of latitude, longitude and height, and interpolate differences of LOS displacements with Surface function of GMT.

(5) Add interpolated differences of LOS displacements to the original interferogram.

One typical example is interferogram for the pair of April 11 and May 27, 2010 for the path 419. Since the time difference is 46 days, little motion is expected. However, we observe LOS changes of ~ 40 cm in the E-W direction. We also find a tongue-shaped region of LOS decrease in the Chugoku district. Applying the above procedure, we obtain interpolated differences of LOS displacement with the opposite sign to the original interferogram. The standard error of difference of LOS displacements for 36 GNSS sites is 7.8 cm. However, the dependences of longitude and latitude are obviously different at 34 N. Therefore we use the Surface function instead of a simple linear function for the interpolation. Finally, we obtain a fairly flat interferogram consistent with the GNSS result. There still remain displacements with shorter wavelength than 20 km, however.

Applying to other pairs, we evaluate standard errors. The minimum is 1.2 cm (Jan. 6 - Feb. 21, 2009), while the maximum is 18.9 cm (May 27 - Jul. 12, 2010). In total 24 pairs, 4 is less than 2 cm, 7 for 2 \sim 4 cm, 6 for 4 \sim 6 cm, 3 for 6 \sim 8 cm, 2 for 8 \sim 10 cm, and 2 is larger than 10 cm. The median is 4.5 cm. For the neighboring path 418 (30 GNSS sites), the minimum is 1.5 cm, while the maximum is 19.8 cm. The median is 4.7 cm. These estimates may give a rough idea of error of PALSAR interferograms including ionospheric disturbances.

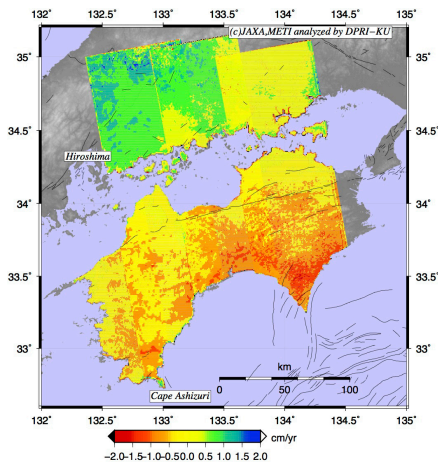
We apply this procedure to other paths (417, 418 and 420) and obtain corrected interferograms that cover the entire Shikoku (Attached figure). This map is fairly consistent with the GNSS velocity field, but there is a discontinuity between the paths 417 and 418. We use interferograms with a rather long perpendicular baseline, which causes decorrelation in mountains. We use only GNSS displacements in plain areas for such interferograms, which results in systematic error.

Keywords: SAR interferometry, PALSAR, ALOS, error, crustal deformation

STT59-10

Room:414

Time:April 29 11:35-11:50



Persistent scatterer SAR interferometry using multi-polarimetric SAR interferograms

ISHITSUKA, Kazuya^{1*} ; TAMURA, Masayuki¹ ; MATSUOKA, Toshifumi¹

¹Graduate School of Engineering, Kyoto University

Persistent scatterer SAR interferometry (PS-InSAR) is a method to estimate surface deformation using a number of SAR interferograms, and has been applied to aseismic fault slip, volcano and land subsidence as a practical monitoring tool. In recent years, more and more satellites that are equipped with SAR, which can acquire multi-polarimetric data has been operated. In this study, we propose a method to processing PS-InSAR analysis using multi-polarimetric SAR interferograms, and show that the estimation accuracy of surface deformation increases.

In this study, we increase estimation accuracy by processing multi-polarimetric SAR interferograms simultaneously. Since, the amount of noise ratio would differ in different multi-polarimetric SAR interferograms depending on the geometry or electromagnetic characteristics of targets, we determine the weighting coefficient between polarimetric SAR interferograms from observed phase based on maximum likelihood method.

We applied the method to ALOS/PALSAR data acquired in multi-polarimetric mode. First, we processed HH-HH and VV-VV interferograms simultaneously. As a result, weighting of HH-HH and VV-VV interferogram was almost identical, suggesting that decorrelation-induced noise in HH-HH and VV-VV interferograms was almost same. In this case, the accuracy of estimated deformation rate would increase twice. On the other hand, when we processed HH-HH and HV-HV interferograms simultaneously, the weighting of HH-HH interferograms are larger than that of HV-HV interferograms, suggesting that HH-HH interferograms has less amount of noise compared with HV-HV interferograms. Nevertheless, we found that the estimation accuracy increases by using both HH-HH and HV-HV interferograms compared with the standard analysis using HH-HH interferograms.

Keywords: persistent scatterer SAR interferometry, surface deformation, polarimetry

Correction by GNSS data for wide area InSAR analysis

MORISHITA, Yu^{1*}

¹GSI of Japan

InSAR results include not only deformation signals but also noises caused by orbital inaccuracies, tropospheric delay and ionospheric delay. Orbital inaccuracies yield a residual orbital phase ramp. As spatial wavelengths of tropospheric and ionospheric noise are typically long, the effect is trivial for a small area but it can be significant for a large area.

Tropospheric noise can be mitigated by estimating the amount of tropospheric delay from a numerical weather model. However, the mitigation does not always work because of the limitation of spatial and temporal resolution of the numerical weather model. There is no common and effective technique to correct ionospheric noise so far while several techniques have been proposed. The ionospheric noise remains a big problem because, in particular, L-band is greatly affected by ionospheric noise. A residual orbital phase ramp can be reduced by flattening the phase in an area with no deformation. Another effective correction method is estimating model parameters (e.g. bilinear surface) to fit other deformation data such as GNSS continuous observation (Tobita et al., 2005; Fukushima and Hooper, 2011). This method works even if the deformation extends the entire area (Kobayashi, 2011). However, if the area is wide, a bilinear surface model is not sufficient because of noises with long wavelengths. A spline interpolation method has been proposed to overcome this problem (Fukushima, 2013).

In this presentation, I will report a GNSS correction technique using a natural interpolation method for scattered points. This technique can mitigate not only residual orbital phase ramps but also noises with long wavelength. Adjusting correction steps enables realistic extrapolations while conventional steps sometimes result in outliers in extrapolated areas. The results of wide area time series InSAR analysis using ALOS/PALSAR data show less noise and more apparent phase changes with shorter wavelength than the interval of the GNSS stations.

References

Tobita, M., H. Munekane, S. Matsuzaka, M. Kato, H. Yarai, M. Murakami, S. Fujiwara, H. Nakagawa and T. Ozawa (2005): Studies on InSAR data processing techniques, Bull. GSI., 106, 37-49 (in Japanese).

Fukushima, Y. and A. Hooper (2011): Crustal deformation after 2004 Niigataken-Chuetsu earthquake, central Japan, investigated by Persistent Scatterer Interferometry, J. Geod. Soc. Japan, 57, 195-214 (in Japanese with English abstract).

Kobayashi, T., M. Tobita, T. Nishimura, A. Suzuki, Y. Noguchi and M. Yamanaka (2011): Crustal deformation map for the 2011 off the Pacific coast of Tohoku Earthquake, detected by InSAR analysis combined with GEONET data, Earth Planets Space, 63, 621-625, 2011.

Fukushima, Y. (2013): Correction of DInSAR noise using GNSS measurements, in proceedings of APSAR 2013, 2013.

Keywords: InSAR, GNSS

Research on the characteristics of ionospheric disturbance around Japan by GPS-TEC for ionospheric correction to InSAR

NAKAGAWA, Hiroyuki^{1*} ; MUNEKANE, Hiroshi¹ ; KUROISHI, Yuki¹ ; KAMIHARA, Masashi²

¹GSI of Japan, ²Pascalina Co.,Ltd

In the monitoring surface deformation using SAR interferometry (InSAR), it is a serious problem that the long-wavelength noise caused by ionospheric disturbance degrades accuracy of the detection of deformation. Since 2013, Geospatial Information Authority of Japan (GSI) have conducted a research project on the method for ionospheric correction to satellite InSAR based on TEC information obtained from two-wavelength observation data of GEONET.

For the first step, in order to understand the characteristics of ionospheric disturbance around Japan, we identified ionospheric disturbance of the period between 2000 and 2011 by GPS-TEC of GEONET and estimate characteristic values of each event.

In the manner in Munekane (2013), we first estimate zenith TEC and TEC gradient in north-south and east-west component every thirty second during the period from GEONET thirty-second RINEX data. Then, we adopted high pass filter of 3600s to remove low frequency component.

Next, based on this GPS-TEC time series, we identified ionospheric disturbance event in the period. In this step, we focus rather on revealing overall trend of ionospheric disturbance than inspecting accuracy of the characteristic value of each event.

The process of identification is as follows. First hourly RMS of TEC was calculated every hour, and, if the number of sites which hourly TEC-RMS is over threshold is more than a certain criterion, regard the epoch as a part of ionospheric disturbance event. Then, viewing the "GEONET GPS-TEC maps over Japan" on the web site of NICT, each disturbance event was divided visually into three category according to the pattern of TEC distribution, "traveling ionospheric disturbance (TID)", "plasma bubble" and "other".

After the identification of event category, we decided characteristics such as event start and end time, affected area and its temporal transition based on ten-minute RMS of TEC. Also, we estimate characteristic values associated with event category such as wavelength of a TID or northernmost latitude of a plasma bubble etc. Finally, we derived characteristics of the ionospheric disturbance around Japan statistically.

We identified 8,815 ionospheric disturbance in the period, reaching maximum of 967 events in 2001, decreasing gradually to minimum of 471 in 2007, and having increasing tendency afterwards. This trend is consistent with solar cycle. The occurrence of TID and plasma bubble is found to be consistent with solar cycle, too.

Also, it appears that TID occurs commonly from May to August, in summer season. TID occurrence also concentrates before and after two hours around 22 o'clock in local time. As for plasma bubble, the occurrence is high from the sunset to midnight in local time. These results are consistent with earlier studies.

References

- Munekane, H., (2013): On ionospheric correction of ALOS/PALSAR interferograms using GEONET data (preliminary report), STT57-09, Japan Geoscience Union Meeting 2013
National Institute of Information and Communications Technology: GEONET GPS-TEC maps over Japan,
http://seg-web.nict.go.jp/GPS/GEONET/index_e.html

Keywords: InSAR, ionospheric disturbance, TEC, GEONET

APPLICATION OF DINSAR TIME SERIES ANALYSIS USING ALOS PALSAR TO EXTERIOR DEFORMATION MONITORING OF DAMS

HONDA, Kenichi^{1*}; MUSHIAKE, Naruo¹; SATOH, Wataru¹; SATOH, Hiroyuki²; KOBORI, Toshihide²; SASAKI, Takashi³; YAMAGUCHI, Yoshikazu⁴; SHIMIZU, Norikazu⁵

¹Kokusai Kogyo Co., Ltd., ²Public Works Research Institute, ³National Institute for Land and Infrastructure Management, ⁴Japan Dam Engineering Center, ⁵Yamaguchi University

The number of aging civil engineering structures is rapidly increasing in Japan. As for dams, it is estimated that 58% of existing dams in the year 2020 will be 50 years old or over after completion. This situation increasingly requires not only efficient deformation monitoring systems for safety management of civil structures but also safe and rapid methods in case of emergencies such as earthquakes.

Remote sensing techniques, especially Synthetic Aperture Radar (SAR), can play an important role to conduct deformation monitoring of civil structures such as dams. Differential Interferometric SAR (DInSAR) analysis using SAR satellite data can be suitable to deformation monitoring in broad areas.

To investigate the applicability of DInSAR analysis for the deformation monitoring, the Taiho Subdam, which is located in the Okinawa Prefecture, Japan, was selected as a study area because the deformation monitoring using GPS have been rigorously conducted since the completion of the dam from December 2006. In this study area, at maximum 114 mm of deformation was measured from December 2006 to December 2010, which corresponds to the observation period by SAR satellite. ALOS PALSAR data, L-band SAR, was used for DInSAR analysis and the results of deformations calculated by DInSAR analysis were compared with the results of the GPS deformation measurements. 28 scenes of ALOS PALSAR data were used: 14 scenes of descending data from December 6, 2006 to December 17, 2010, and 14 scenes of ascending data from January 12, 2007 to January 23, 2011, respectively.

The values of deformations calculated by DInSAR analysis were about 70 or 80% of those measured by GPS during observation period about four years. Although the DInSAR analysis results were expected to have some errors and were different from the GPS measurement results to some extent, DInSAR deformation monitoring is sufficient enough to monitor few-centimeter deformations. Additionally time series changes by DInSAR analysis can well reproduced the tendency of the settlement of the dam. This indicates a possibility that DInSAR analysis is useful for the deformation monitoring for civil structures.

Keywords: Dam, Exterior deformation monitoring, DInSAR, SBAS, GPS

Approach for monitoring ground deformation around the active volcanoes in Japan by InSAR time series analysis

MIURA, Yuji^{1*} ; ANDO, Shinobu² ; NAKAMURA, Masamichi¹

¹Volcanological Division, JMA, ²MRI

In previous studies, we have reported the analysis results about domestic active volcanic areas using D-InSAR of ALOS since 2007. In recent years, InSAR time series analysis technique has been developed. Therefore various studies have been reported for monitoring ground deformation using InSAR time series analysis. In this study, we have applied this procedure to the analysis of the data of ALOS/PALSAR for monitoring ground deformation of the active volcanoes in Japan.

As a result, we can detect ground deformations associated with volcanic activities of Tokachidake, Azumayama, Izu-Oshima, Miyakejima, Satsuma-Iojima and others. These obtained ground deformations by InSAR time series analysis were basically consistent with the results of GPS.

Keywords: InSAR time series analysis, ground deformation, ALOS/PALSAR, active volcano

Surface displacement around Hachobaru geothermal field inferred from persistent scatterer SAR interferometry

ISHITSUKA, Kazuya^{1*} ; TSUJI, Takeshi² ; MATSUOKA, Toshifumi¹ ; FUJIMITSU, Yasuhiro³ ; NISHIJIMA, Jun³

¹Graduate School of Engineering, Kyoto University, ²International Institute for Carbon-Neutral Energy Research (I2CNER), Kyushu University, ³Faculty of Engineering, Kyushu University

Fluid migration around geothermal field can cause surface displacement. Leveling campaign and GPS measurement has been used to estimate surface displacement and shown the usefulness for reservoir monitoring at geothermal field. Recently, persistent scatterer SAR interferometry (PS-InSAR) analysis has been developed as a practical tool for surface displacement monitoring. By making use of the advantage of wide data coverage of satellite image, the analysis enables us to estimate surface displacement at the whole geothermal field with high spatial density. In this study, we applied PS-InSAR analysis on areas around Hachobaru geothermal field, the largest geothermal field in Japan, located Kyushu Island. For the analysis, we used 18 ALOS/PALSAR images acquired from July 2007 to December 2010 from an ascending orbit.

As a result of the analysis, we estimated secular surface displacement with the maximum rate of 15 mm/year opposite to satellite direction, which can be inferred as ground subsidence. We also found temporally irregular displacement along with the secular displacement. This irregular displacement has occurred all of Mt. Kuju, suggesting that displacement at Mt. Kuju has influenced displacement at the geothermal field. Moreover, we found that the secular displacement has decayed over time and has clear boundaries which possibly correspond to fault locations.

Keywords: surface displacement, persistent scatterer SAR interferometry, Hachobaru geothermal area

The Steady Crustal Deformation Analysis in Tokai region by InSAR

ANDO, Shinobu^{1*} ; IWAKIRI, Kazuhiro² ; AOKI, Gen²

¹MRI, ²JMA

ALOS has an L-band SAR (PALSAR), which is of help to understand of a ground surface state, and its interferometric coherence is highly effective for the crustal deformation observation.

We analyzed the ALOS/PALSAR data around Omaezaki and Kakegawa cities in Shizuoka Prefecture, and tried to detect steady crustal deformation due to the subduction of the Philippine Sea plate. In this study, in order to obtain steady-state deformation (time series), we subjected to interference processing on the image pairs of a number of different imaging date interval. Then, using a variation of the satellite line-of-sight direction in the interference each images and we were calculated the average variation of the 46 days (stacking process). However, to reduce noise, we analysed except for some interferograms with obvious noise. This method can be expected to improve detection accuracy, because of able to reduce the influence of noise caused by the ionosphere.

We used 23 ascending data acquired from January 2007 to October 2010 and 19 descending data acquired from October 2006 to September 2010. Before solving for the displacement time series, we corrected the atmosphere phase delay by Japan Meteorological Agency nonhydrostatic model (JMA-NHM), and calculated the displacement of the satellite line-of-sight direction of the pair of all. The average displacement of the satellite line-of-sight direction of the 46 days was calculated under the assumption that the variation in the period of each pair is constant. The distance between the imaging date is different for each pair, but we did not weight during the averaging process.

As a result, steady-state deformation was hardly observed in the analysis of the ascending orbit data, but in the analysis of the descending orbit data, were observed the steady-state deformation the away from the satellite in the radar line-of-sight direction. This crustal deformation was significant in Omaezaki area, especially. These results are consistent with the displacement vector by GNSS. In this report, we also reported about InSAR time series analysis using *StaMPS* program was developed by the Stanford Institute of Technology.

Some of PALSAR data were prepared by the Japan Aerospace Exploration Agency (JAXA) via the Geospatial Information Authority of Japan (GSI) as part of the project "ALOS Domestic Demonstration on Disaster Management Application" of the Earth Working Group. Also, we used some of PALSAR data that are shared within PALSAR Interferometry Consortium to Study our Evolving Land surface (PIXEL). PALSAR data belongs to Ministry of Economy Trade and Industry (METI) and JAXA. We would like to thank Dr. Shimada (JAXA) for the use of his *SIGMA-SAR* software. In the process of the InSAR, we used "the digital elevation map 50m-mesh" provided by GSI, and Generic Mapping Tools (P.Wessel and W.H.F.Smith, 1999) to prepare illustrations.

Keywords: InSAR, Ground deformation, ALOS/PALSAR, Tokai region

Monitoring of Sakurajima Volcano using Cosmo-SkyMed

MIYAGI, Yosuke^{1*} ; OZAWA, Taku¹ ; SHIMADA, Masanobu²

¹National Research Institute for Earth Science and Disaster Prevention, ²Japan Aerospace Exploration Agency

Sakurajima volcano is located in southwestern part of Japan, and currently a most active volcano in Japan. Eruptive activities from Showa-crater have activated since 2009, and several explosive eruptions occurred in 2012. On July 24, 2012, another large eruption occurred from Minamidake-crater after a lapse of 18 months. To understand current condition and future unrest of Sakurajima, periodic monitoring is required. Although it is generally difficult to make a field observation in dangerous active volcanoes, a satellite remote sensing can make observations of even ongoing volcanoes periodically. Especially, Synthetic Aperture Radar (SAR) sensor is well-suited for monitoring active volcanoes because it can penetrate ash clouds and can observe targets like an active vent. Moreover, SAR data are applicable to use a Differential Interferometric SAR (DInSAR) technique to detect crustal movement associated with the magmatic activities. In this study, we used COSMO-SkyMed data for monitoring Sakurajima volcano and tried DInSAR processing. Monitoring using high-resolution amplitude images revealed changes of backscattering intensity probably due to some kind of surface change within or around the crater. DInSAR processing suffered from low coherence, therefore we acquired quite limited geodetic information.

Keywords: SAR, Sakurajima, Deformation

Volume Increase of Lava within the Kirishima, Shinmoe-dake Crater, Detected by TerraSAR-X/DInSAR

MIYAGI, Yosuke^{1*} ; OZAWA, Taku¹ ; KOZONO, Tomofumi² ; SHIMADA, Masanobu³

¹National Research Institute for Earth Science and Disaster Prevention, ²Department of Geophysics, Graduate School of Science, Tohoku University, ³Japan Aerospace Exploration Agency

Shinmoe-dake in the Kirishima volcano group is located in southwestern part of Japan. In January 2011, eruptive activities started from the Shinmoe-dake crater with a rapid accumulation of lava within the crater. The eruption phase ceased by the beginning of September, and the post-eruptive inflation also ceased by November 2011. After the 2011 eruption, monitoring by TerraSAR-X have continued and revealed a continuous shortening of satellite-ground distance even after the end of the main activity. This LOS shortening means uplifts of the lava surface. We estimated the volume increase of the lava after November 2011, using DInSAR processing of TerraSAR-X data, and concluded that the volume increase still continued in January 2014. The volume change rate has exponentially decreased with a small fluctuation as an overall trend. PSInSAR and long-term DInSAR results show LOS elongation including a subsidence in the northeast flank of the crater. It is interpreted that the subsidence is caused by deflation of a shallow deformation source located just beneath the crater. A total amount of effused lava after November 2011 is comparable to a volume decrease of the shallow source estimated from the deflation deformation. This long-term continuous lava extrusion suggests a possibility of an additional injection from the deeper source.

Keywords: SAR, Kirishima, Shinmoe-dake, Deformation

Crustal deformation in Izu-Oshima Island detected by PS-InSAR analysis and estimation of volcanic deformation source

HASEGAWA, Yuichi^{1*} ; TABELI, Takao² ; OZAWA, Taku³

¹Grad. School Int. Arts Sciences, Kochi Univ., ²Fac. Science, Kochi Univ., ³National Research Institute for Earth Science and Disaster Prevention

Mt. Mihara in Izu-Oshima Island have erupted 21 times in the last 800 years. The latest eruption occurred in 1986 inside the caldera. Though spatially and temporally dense observation network is desired to continuously monitor volcanic activities, it is not easy to construct such a network in a mountainous region. In this study, we conduct time-series analysis of ALOS/PALSAR images over Izu-Oshima Island using persistent scatter interferometric SAR (PS-InSAR) method to detect volcanic deformation.

From the analysis of 20 images collected from ascending track during the period from October 2007 to February 2011, we detect distance change of about 15 cm extension in the line-of sight (LOS) direction inside the caldera. Similarly the extension of about 14 cm is detected at the same location from the analysis of 18 images from descending track during the period from January 2007 to March 2010. Next we compare the LOS distance changes with those converted from GPS coordinate time-series at four continuous sites in the island. The RMS between them are as large as 1.3-3.2 cm, implying that SAR results are good enough to monitor volcanic deformation over the island.

Combining the LOS distance changes from the ascending and descending tracks, we derive quasi-vertical and quasi-east-west components of the displacement. The most remarkable is the vertical displacement of the caldera where the subsidence of about 16 cm is detected during 2007-2010 with small occasional uplifts. Moreover uplift of about 11 cm is recognized in the eastern coastal area of the island during the same period. Based on the quasi-vertical component of the displacement, we estimate a spherical pressure source model (Mogi, 1958) below the island. We assume two sources with different depth and estimate the optimum model using a grid search method. Horizontal position of the shallower source is fixed to coincide with the location of the caldera and its depth is varied every 0.5 km in a range of 2.0-4.5 km. Horizontal position of the deeper source is varied every 2 km and its depth is checked every 0.5 km in a range of 5.0-10 km. The optimum model shows that the shallower source is located at a depth of 3.0-4.5 km where inflation and deflation are occurring alternatively while the deeper source is located at a depth of 6.0-9.0 km where nearly constant inflation rate of about 8 million m³ per year is expected. These results can be interpreted that the deeper magma reservoir continues to expand due to magma supply from the mantle while the shallower reservoir is affected by magma supply from the deeper source and gravitational load of lava that spreads within the caldera.

Keywords: PS-InSAR method, time-series analysis, Izu-Oshima Island, crustal deformation, volcanic deformation source

Flow velocity measurements of ice streams in the southern part of Soya Coast, Antarctica, by DInSAR

SHIRAMIZU, Kaoru^{1*} ; DOI, Koichiro² ; AOYAMA, Yuichi²

¹The Graduate University for Advanced Studies, ²National Institute of Polar Research

Differential Interferometric Synthetic Aperture Radar (DInSAR) is an effective tool to measure flow rate of ice streams on Antarctic continent. In this study, we applied the DInSAR technique to L band (wavelength 23.6cm) SAR data acquired by ALOS/PALSAR, and tried to measure flow velocity around Skallen, in the southern part of Soya Coast, East Antarctica. We used 9 scenes (Path633, Row 571-572), observed during the period from November 23, 2007 through January 13, 2010. In order to remove topographic fringes in the interferograms, we used a digital elevation model ASTER GDEM.

According to the analysis, ice flow rate of up to 3.5cm/day was obtained in the line of sight direction. Although no displacement is expected in areas of outcrops in general, we found displacements up to 37cm in the outcrops of obtained displacement maps. These displacements are considered to be apparent ones and must contain errors induced in the process of analysis. Therefore, it is possible to use apparent changes as a measure of the error contained in ice flow rate estimation.

In this presentation, we will show the results of flow rate estimation of the ice streams, and discuss the errors included in the flow rate estimation.

Keywords: Differential Interferometric SAR, Antarctic ice sheet, ice stream

Flow measurements of ice sheets in Arctic region by differential SAR interferometry

DOI, Koichiro^{1*} ; YAMANOKUCHI, Tsutomu³ ; NAKAMURA, Kazuki⁴ ; SHIRAMIZU, Kaoru²

¹National Institute of Polar Research, ²The Graduate University for Advanced Studies (SOKENDAI), ³RESTEC, ⁴Nihon University

Rapid ice sheet mass losses from ice sheets have been found in Greenland and the Canadian Arctic Archipelago on and after 2000 from the observations by the satellite gravity mission GRACE (Svendsen et al. 2012, Gardner et al. 2011). It is considered to be one of the causes that flow rate of ice sheet and ice stream was accelerated and ice mass outflow into the sea increased.

We aim to measure flow rates of ice sheet and ice streams in the Arctic region by applying differential Synthetic Aperture Radar (SAR) interferometry (DInSAR) with a digital elevation model ASTER GDEM to satellite SAR data. In addition, we intend to explore whether changes in the flow rate happen or not.

We obtained displacement maps along line of sight direction for 46 days of three regions in north eastern Greenland and Ellesmere Island of northern Canadian Arctic Archipelago observed by ALOS/PALSAR by applying differential SAR interferometry. We will show the obtained displacement maps in the presentation, and will also intend to discuss changes in the flow rates by applying three or four pass interferometry.

Keywords: Differential SAR interferometry, flow, ice sheet, Arctic region

Spatial distribution and classification of rock glaciers in Kyrgyz Ala-Too Range, Central Asia

YAMAMURA, Akiko^{1*} ; NARAMA, Chiyuki¹ ; TOMIYAMA, Nobuhiro² ; TADONO, Takeo³

¹Niigata University, ²RESTEC, ³JAXA

In the arid and semi-arid region of Central Asia, Tien Shan Mountains is known as important water tower in Central Asia. Although the current situation of mountain glaciers and permafrost should be researched for estimate of water resources, mountain permafrost is not clarified in the Tien Shan (Marchenko et al., 2007; Sorg et al., 2012). In recent years, landslides caused by the melting of mountain permafrost in Ak-Shiyrak mountains, show that recent changes of mountain permafrost begin to influence to mountain environment including the disaster. In this study, to clarify mountain permafrost environment, we researched spatial distribution and classification of rock glaciers in Kyrgyz Ala-Too Range, Tien Shan Mountains. In addition, we applied InSAR analysis to the ALOS PALAR data obtained in 2007-2010, to research moving of rock glaciers. We extracted polygon data of rock glaciers based on aerial photo interpretation and ALOS PRISM, using ArcGIS. Rock glaciers were classified an active and inactive-fossil types by NDVI (Normalized Difference Vegetation Index) of ALOS AVNIR-2 and field observation in the summer 2013. The distributions of active rock glaciers show the lower limit of mountain permafrost is 3300m in the northern part and 3500m in the southern part of the Kyrgyz Ala-Too Range. We confirmed moving of some rock glaciers in this mountain area using InSAR analysis. In particularly, the moving of rock glaciers in the southern part of the range is remarkable. The most of these active rock glaciers developed from glacier ice. We report the results in detail in JpGU meeting.

Keywords: mountain permafrost, rock glacier, InSAR, ALOS PALSAR, Tien Shan Mountains

Development of InSAR processing tools in NIED ?Part3?

OZAWA, Taku^{1*}

¹National Research Institute for Earth Science and Disaster Prevention

Synthetic aperture radar (SAR) became one of the useful tools for crustal deformation detection. Recently, InSAR processors which can be used freely in scientific research (e.g., ROI_PAC, GMTSAR, and Doris) were released, and enabled anyone to do crustal deformation detection by InSAR. Especially, algorithm of two-pass differential InSAR analysis matured, and it enabled anyone to obtain almost same results. On the other hand, advanced InSAR analysis methods, e.g., time-series analysis, have been recently used to detect precise crustal deformation. However, many issues to improve remains in such analyses. In order to research on improvements for such analysis, we are developing InSAR processor.

In this InSAR processor, general procedure is adopted. (1) Format conversion of SLC and creation of parameter files. (2) Rough co-registration of two SLCs considering parallel shift only. (3) Estimation of affine transformation coefficients. (4) SLC resampling. (5) Generation of the initial interferogram. (6) Simulation of a SAR intensity image and estimation of translation tables between geodetic and radar coordinates based on DEM. (7) Co-registration between simulated and observed SAR intensity images. (8) Correction of translation tables. (9) Simulation of the orbital and the topographic phase components. (10) Generation of differential interferogram. (11) Applying interferogram filter. (12) Geocoding.

In JPGU meeting 2013, we showed comparison between results from our processor and from GAMMA SAR processor. Although their results were roughly the same, it indicated that many improvement points remained. In 120th meeting of the Geodetic Society of Japan, we presented about improvement of coherence by the spectrum shift filter (Gatelli et al., 1994), improvement of calculation speed, and correspondence to skewed images. After that, this processor corresponded to the InSAR processing with FBS-FBD image pair of ALOS/PALSAR using SLC over-sampling and band-pass filter. We added DEM resampling function by over-sampling method and by the bi-cubic spline interpolation. Furthermore, we are attempting to improvement of the image matching now. After this correspondence, the first step of this development will be finished. In next step, we will attempt more improvements and additions of other advanced algorithms.

Keywords: SAR, InSAR, software, tool